İmalat Teknolojileri ve Uygulamaları
Cilt: 5, No: 2, 2024 (65-74)
Araştırma Makalesi
e-ISSN: 2717-7475

Manufacturing Technologies and Applications
Vol: 5, Issue: 2, 2024 (65-74)
Research Article
e-ISSN: 2717-7475

Detecting Manufacturing Defects on Printed Circuit Boards Using Metamaterial-Based Circular Microstrip Patch Antenna

Sultan Suheyla Bakir[1,2*], Asaf Behzat Sahin[2]

[1]*Turkish Aerospace, Ankara, Türkiye*
[2]*Ankara Yıldırım Beyazıt University, Department of Electrical and Electronics Engineering, Ankara, Türkiye*

ARTICLE INFORMATION

Received: *30.04.2024*
Accepted: *25.06.2024*

Keywords:
Printed circuit boards
Metamaterials
Circular patch antenna
Non-Destructive testing
Sensors

ABSTRACT

This study introduces a novel all-signal-processing based printed circuit boards (PCB) defect detection tool. A microstrip circular patch antenna is designed having a metamaterial-based (MTM) ground plane to detect manufacturing defects of short circuits and open circuits on PCB. In that regard, PCB specimens of FR-4 as the substrate and copper microstrip lines as the conductive wiring lines are designed and manufactured. Five vertical copper lines printed side by side on the top of the substrate are used to demonstrate the working mechanism of the designed antenna sensor. Two different defect scenarios of open and short circuits with controlled locations are studied to determine variations in the return loss data of the proposed structure. Antenna return loss behaviors in terms of the locations of the faults are employed to prepare a database to detect not only the presence of the faults but also determine their locations. The designed metamaterial based circular patch antenna can be used successfully to determine not only the fault type but also the location of the fault within mm-range on the PCB board. Depending on the fault location, the resonance frequency as well as the return loss magnitude variation from -40dB to -16 dB around 1.5 GHz can be used for the sensing operation on PCB faults. Since the samples to be measured are not irreversibly damaged during the testing process, the proposed design can be considered a non-destructive measurement method to provide information about the type and location of defects with real-time measurement data.

Metamalzeme Tabanlı Dairesel Mikroşerit Yama Anteni Kullanılarak Baskı Devre Kartlarındaki Üretim Hatalarının Tespiti

MAKALE BİLGİSİ

Alınma: *30.04.2024*
Kabul: *25.06.2024*

Anahtar Kelimeler:
Baskılı devre kartı
Metamalzemeler
Dairesel yama anten
Tahribatsız muayene
Sensörler

ÖZET

Bu çalışmada, baskılı devre kartları (PCB) üzerindeki kısa devre ve açık devrelerden kaynaklanan imalat hatalarını tespit etmek için metamalzeme tabanlı (MTM) yer düzlemine sahip bir mikroşerit dairesel yama anteni tasarlanmıştır. Bu bağlamda altlık olarak FR-4 PCB numuneleri ve iletken kablolama hatları olarak bakır mikroşerit hatları tasarlanıp üretilmektedir. Alt tabakanın üst kısmında yan yana basılmış beş dikey bakır çizgi, tasarlanan anten sensörünün çalışma mekanizmasını göstermek için kullanılmıştır. Önerilen yapının geri dönüş kaybı verilerindeki değişiklikleri belirlemek için konumları kontrollü açık ve kısa devrelerden oluşan iki farklı arıza senaryosu incelenmiştir. Tasarlanan ve üretilen sensörün daha yüksek hassasiyetini elde etmek için, sekizgen bir halka ile çevrelenmiş çapraz çizgili MTM hücre yapıları, önerilen antenin yer düzleminin bir parçası olarak periyodik olarak yerleştirilmektedir. Arızaların konumlarına göre anten geri dönüş kaybı davranışları, arızaların sadece varlığını tespit etmekle kalmayıp aynı zamanda konumlarını da tespit etmek için bir veri tabanı hazırlamak amacıyla kullanılmıştır. Ölçülecek numuneler test sürecinde geri dönülemez bir hasara uğramadığından, önerilen tasarım, gerçek zamanlı ölçüm verileriyle kusurların türü ve konumu hakkında bilgi sağlayan, tahribatsız bir ölçüm yöntemi olarak değerlendirilebilir.

** Corresponding author, e-mail: s.suheylayilmazz@gmail.com*
To cite this article: S.S. Bakir, A.B. Sahin, Detecting Manufacturing Defects on Printed Circuit Boards Using Metamaterial-Based Circular Microstrip Patch Antenna, Manufacturing Technologies and Applications,5(2), 65-74, 2024.
https://doi.org/10.52795/mateca.1475763, This paper is licensed under a CC BY-NC 4.0

1. INTRODUCTION (GIRIŞ)

Today's continuously improving technology and digitalization concepts have brought an ever-increasing usage of electronic devices through printed circuit boards (PCBs). The PCBs are thin boards made of insulating materials providing conductive wiring/pathways to connect various components [1]. PCBs are acknowledged as the main structures for electronic devices by properly combining electronic components. The demand for utilizing PCBs in all electronic structures has increased rapidly because of low costs, compact sizes, low electronic noise, stable production/performance, and durability [2]. Because of their increasing usage portfolio in related industries and consumer electronics, the risk of having defects on PCB cards becomes unavoidable. Any defect types on a PCB may affect the performance of electronic devices negatively as much as causing the devices not to function.

Unlike the importance and complexity of the defects on PCBs, determining these defects can be challenging through traditional methods. For this reason, identifying and repairing PCB defects at early manufacturing stages has become a critical topic in engineering and production processes.

Defects on PCBs refer to all defects/faults that occur in PCBs during the manufacturing process, from minor issues to major faults. It is crucial to identify these defects to maintain reliability and quality in line with various industry guidelines and reduce operational costs in the long run. The most common defect types are open and short circuits, insufficient or excessive soldering and paste, and missing through holes and components [3].

Open circuits affect the flow of electric current due to discontinuities in conductor paths/wirings. Unintended connections between individual conductor paths are known as short circuits and cause diversion of electric current. Other defects of inadequate/excessive solder or solder bridges may affect the electrical connections between components, eventually causing circuit failures.

High-tech PCB defect inspection techniques have recently become more reliable. Automated optical inspection (AOI), high-resolution cameras augmented with advanced image processing algorithms is used to identify surface faults quickly and with high accuracy [4, 5]. The AOI is a contactless verification approach using an image-processing algorithm to analyze failures through individual PCB layers on images. The image-processing tool evaluates the image as compared to an error-free image based on pre-determined error types. X-ray inspection methods of computed tomography (CT) are helpful to identify internal defects in more detail [6, 7]. Through this technique, internal forms and structural compositions are assessed through a non-destructive scheme. X-ray sources are used with respect to light sources of AOI. Machine learning (ML) and artificial intelligence (AI) have recently been used for detection accuracy and defect inspection [8,9]. With the help of convolutional neural network (CNN) algorithms, deep learning methods are enable to detect various defect types as well as organize them via image classification. However, these PCB defect inspection techniques have some limitations. For example, X-ray methods are time-consuming, optical methods are merely used for surface-based defects, and AI tools are not optimized for use with annotated data.

Thus, this study proposes a real-time, non-destructive, and accurate measurement method for detecting various PCB faults through a novel all-signal-processing-based technique. With this approach, the return loss of the antenna is measured using a network analyzer, which can be both vector and scalar. Depending on the fault location and type, the magnitude and/or operating frequency point is measured and correlated with the fault on PCBs. Since there are distinct differences between the antenna responses due to the fault, the system can estimate the fault location, size, and depth with high accuracy in real-time measurement.

2. MATERIAL AND METHOD (MATERYAL VE YÖNTEM)

In this study, a microstrip patch antenna is used. Such antennas conventionally consist of a patch, a dielectric layer with a known thickness value, and a conductive ground plane placed at the backside of the dielectric layer. Even though the patch can be in any shape including square or rectangular, we use a circular patch since it provides higher bandwidth, omnidirectional pattern due

to circular symmetry, lower cross-polarization, and less side lobe power compared to rectangular patch antennas.

2.1. Antenna and MTM Design (Anten ve MTM Tasarımı)

In order to calculate the operating frequency of the circular patch antenna, the fundamental resonance mode corresponding to circular patch should be initially considered. The resonance frequency of the fundamental mode of the circular microstrip patch antenna can be expressed as in (Eq.1):

$$f = \frac{c}{2\pi R\sqrt{\varepsilon_{eff}}} \tag{1}$$

In this formula c is the speed of light in vacuum or free space, R is the radius of the circular patch, and ε_{eff} is the effective permittivity of the microstrip line which can be approximated as in (Eq.2):

$$\varepsilon_{eff} = \frac{\varepsilon_r+1}{2} + \frac{\varepsilon_r-1}{2}\left(1+\frac{10h}{R}\right)^{-\frac{1}{2}} \tag{2}$$

Here, ε_r is the relative electrical permittivity of the substrate and h is the substrate height. If we the effective permittivity is substituted into the formula for resonance frequency, the following can be obtained as in (Eq.3):

$$f = \frac{c}{2\pi R\sqrt{\frac{\varepsilon_r+1}{2}+\frac{\varepsilon_r-1}{2}\left(1+\frac{10h}{R}\right)^{-\frac{1}{2}}}} \tag{3}$$

One can simply found the radius of the patch using the equation above as in (Eq.4):

$$R = \frac{c}{2\pi f}\sqrt{\frac{\varepsilon_r+1}{2} + \frac{\varepsilon_r-1}{2}\left(1+\frac{10h}{R}\right)^{-\frac{1}{2}}} \tag{4}$$

This expression is complicated to solve due to the presence of another R in the equation. Therefore, this is normally solved iteratively or via use of numerical methods.

The structure designed and manufactured in this study is composed of a microstrip patch antenna in circular shape made with copper of a thickness of 0.035 mm. The copper thickness is the standard thickness value commonly used for printed circuit boards having FR4 substrate. The designed copper patch is placed on a dielectric layer, FR-4, with a thickness of 1.6 mm. In order to design the antenna structure to operate at a desired frequency, the radius of the patch should be calculated. Considering that R refers to the patch radius and h is the substrate thickness, then the radius can be calculated using the f_r resonance frequency and ε_r the dielectric constant of the substrate (FR-4) as in (Eq.5) [10]:

$$R = \frac{F}{\sqrt{1+\frac{2h}{\pi\varepsilon_r F}\left[ln\left(\frac{\pi F}{2h}\right)+1.7726\right]}} \tag{5}$$

In this equation, $F = \frac{8.791\text{x}10^9}{f_r\sqrt{\varepsilon_r}}$ is associated with the relative permittivity and the operating frequency. The radius R of the circular patch was optimized and found to be approximately 26 mm for the frequency point of f= 1.8 GHz. For this optimization, the sensitivity of the LPKF Protomat prototype builder which is 0.1 mm. This prototype builder machine is used to manufacture the proposed metamaterial based antenna structure. Since the metamaterial lines and cells need to be thick enough to be manufactured, 0.48 mm thickness is selected after a few manufacturing trials. Lower thickness values for the metamaterial lines cannot be successfully produced. After obtaining the most appropriate metamaterial line thickness value, the cell structure was simulated and the

operating frequency is determined. At the last step, radius of the circular patch of the antenna is tuned by using parameter sweep technique that comes with the CST Microwave Studio software.

After obtaining the detailed dimensions of the microstrip patch antenna in a circular shape, a metamaterial cell structure that will be used with the same layer of the ground plane can be designed. Metamaterials are man-made materials providing unusual properties such as negative refractive index that cannot be obtained using natural materials. The idea of having a negative refractive index, meaning negative electrical permittivity and negative magnetic permeability, originated from the work of Victor Georgievich Veselago, a famous Russian physicist [11]. To increase the sensitivity of the designed structure, the following MTM cell structure was designed and optimized using an electromagnetic simulation tool. The detailed dimensions of the finalized MTM structure are given in the following figure (Fig. 1). As seen in the figure, the structure is composed of three vertically and three horizontally placed lines surrounded by an octagonal ring. The complete reflecting part of the structure is designed by copper with a thickness of 0.035 mm, and FR-4 dielectric with a permittivity (ε_r) of 4.3 with a thickness value of h=1.6 mm is used as the substrate.

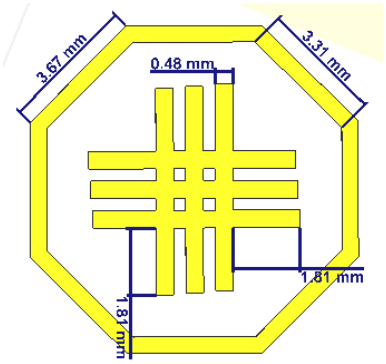

Figure 1. Metamaterial cell structure with detailed dimensions (Detaylı boyutlarda metamateryal hücre yapısı)

The designed MTM cell structures are then placed on the background layer of the circular patch antenna. A total of 25 cell structure is placed at the ground plane for more sensitivity. The detailed dimensions of the structure are given in the figure below (Fig. 2).

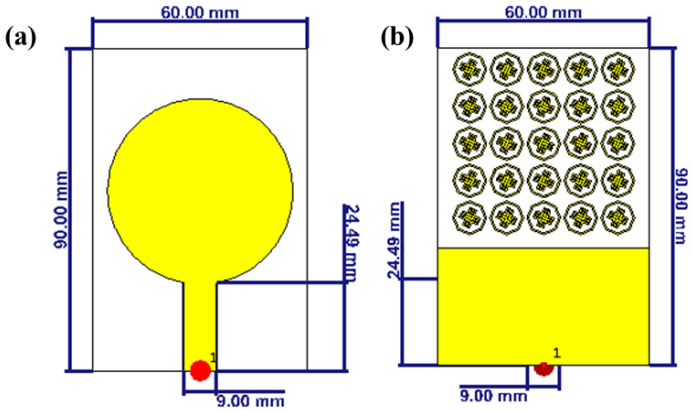

Figure 2. Front-side (a) and back-side views (b) of the MTM based circular patch antenna (MTM tabanlı dairesel yama anteninin önden (a) ve arkadan görünümleri (b))

Following the simulations, the antenna is manufactured along with the PCB boards used for different fault scenarios, which can be seen in Fig. 3. To manufacture the designed configuration, FR-4 substrate is used for the dielectric layers while copper is used for the conductive layers for all the configurations. LPKF Protomat prototype builder is used for this process.

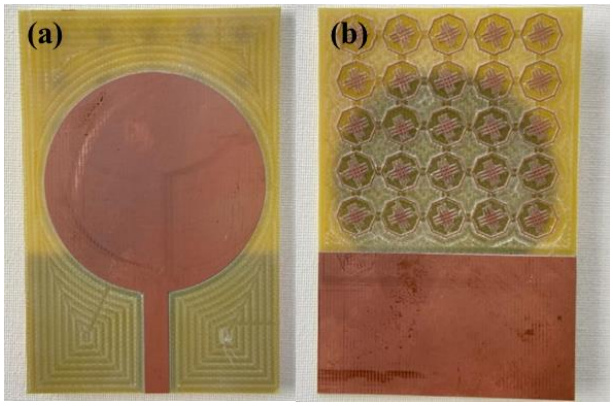

Figure 3. Front-side (a) and back-side (b) of the manufactured MTM based circular patch antenna (Üretilen MTM tabanlı dairesel yama antenin ön yüzü (a) ve arka yüzü (b))

2.2. PCB Fault Scenarios (PCB Arıza Senaryoları)

In this part, a PCB board with five straight copper lines is placed at the back side of the antenna across the ground plane and MTM cells. The PCB board is tested according to three scenarios; no-fault, open circuit, and short circuit cases. To clearly illustrate the working mechanism of the proposed structure, faults are made of all copper lines as demonstrated in the following figures (Fig. 4 and Fig.5).

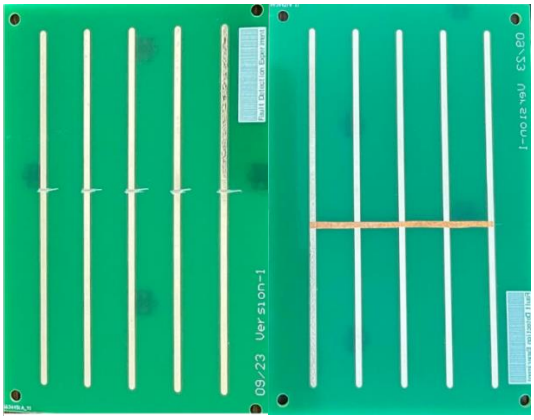

Figure 4. PCBs with open circuit fault (left) and short circuit fault (right) (Açık devre arızalı (solda) ve kısa devre arızalı (sağda) PCB'ler)

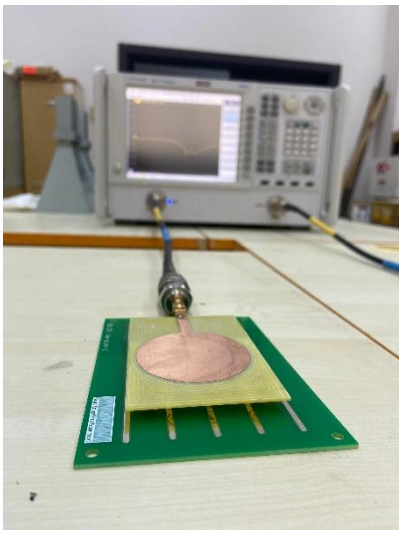

Figure 5. Measurement setup demonstrating the network analyzer, antenna, and PCB sample (Ağ analizörünü, anteni ve PCB örneğini gösteren ölçüm kurulumu)

3. EXPERIMENT AND OPTIMIZATION RESULTS (DENEY VE OPTİMİZASYON SONUÇLARI)

Although numerous defect types can be encountered on PCBs, this study focuses on two scenarios of open circuit and short circuit cases. Initially, the results of the error-free PCB board is given below in Fig.6. In both cases, open and short circuit lines are made using seven different locations starting from the center of the electronic board. The board is prepared using five vertical lines with 2 mm of width and 0.035 mm of thickness using copper. Through employing an optimization program, detection of the exact size, depth, type, and location of various defect types will be one of our future studies since it will require numerous samples and simulations to fill a necessary database.

For the experimental tests, a vector network analyzer is used to obtain scattering parameters, also known as S-parameters. Since we only used one port, obtaining S11 (Reflection) is sufficient. For this reason, only the signal sent and received from the same port (Port-1) in terms of frequency (GHz) is used for the measurements in both fault scenarios. In order to eliminate the cable loss and the adapter effects, the VNA is calibrated using a calibration kit including Short, Open and Load apparatus for the corresponding frequency range.

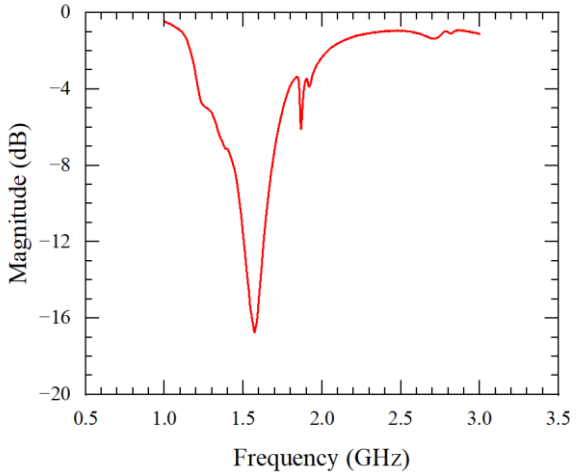

Figure 6. Return Loss of the PCB without any physical faults/defects (Herhangi bir fiziksel arıza/kusur olmadan PCB'nin geri dönüş kaybı)

3.1. Open Circuit Case (Açık Devre Durumu)

A total of 7 different variations of each are used for both open and short circuit cases where location of the defect is shifted from 0 to 18 mm by 3 mm of increments. For the open circuit case, a horizontal cut is made for all vertical lines with seven different locations (Fig. 7). To use the designed structure as the sensor for detecting PCB faults, the return loss (S11) behavior of the design should provide a linear variation depending on the fault type and location. For this purpose, the simulation and experimental studies are performed, and the results are presented in Fig. 8 and Fig. 9, respectively.

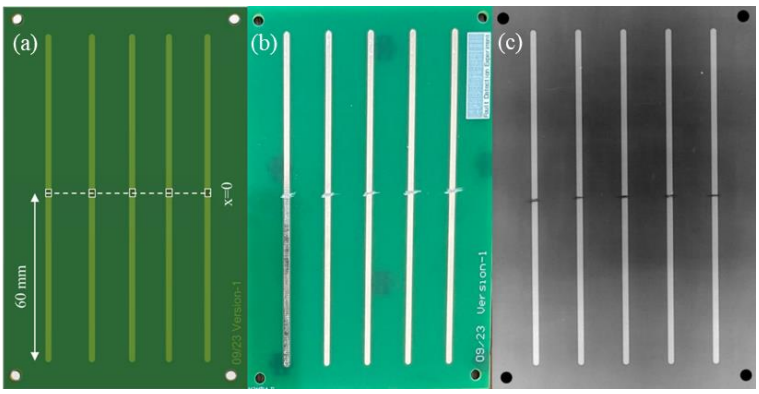

Figure 7. The design representation of the PCB (a), image of the PCB with open-circuit defect at x=0 (b), and X-ray image of the PCB with open-circuit defect at x=0 (c).

The straight horizontal cuts were made on the vertical lines for different locations from x=0 (center of the PCB) to x=18 mm.

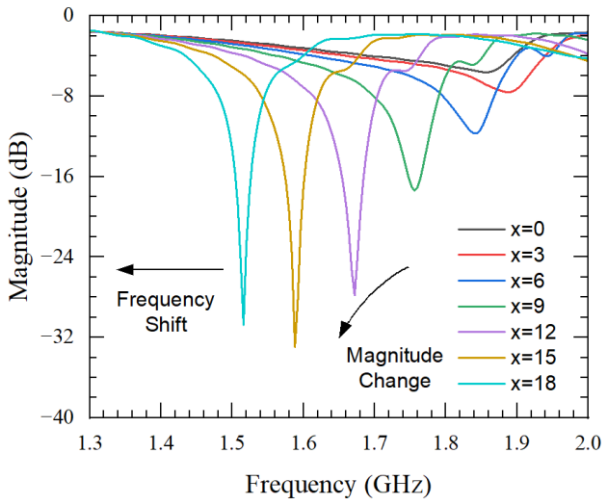

Figure 8. Simulation results for the Return Loss Behavior with respect to different locations of open circuits (Açık devrelerin farklı konumlarına göre geri dönüş kaybı davranışı için simülasyon sonuçları)

The simulation is conducted by adding 1mm thick cuts on the lines, and the results are shown above. As can be seen in the figure, not only the resonance frequencies but also the amplitudes of the return loss curves change depending on the fault location. This change is almost linear providing a sensitive determination function for the PCB fault location. In addition, experimental studies are performed using the manufactured antenna and the PCBs using a Vector Network Analyzer (VNA) capable of measuring 0-43 GHz. The obtained results for all locations are drawn in the following figure (Fig. 9). As seen in the figure below, the resonance frequency points shift left to lower frequency points as the location of the open circuit fault increases to higher values. This behavior is also observed in the simulation results with only small margins. The differences might be caused by laboratory conditions, manufacturing tolerances, and calibration errors. However, the overall behavior is almost the same, and the shift amount in the frequency is almost linear like the simulations.

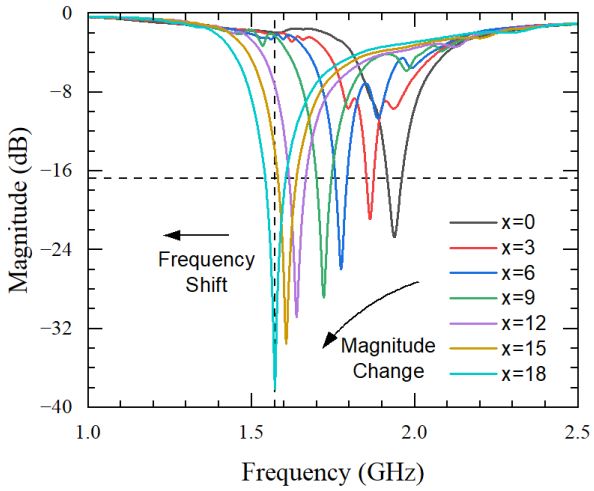

Figure 9. Experiment results for the Return Loss Behavior due to different locations of open circuits (Açık devrelerin farklı konumlarından kaynaklanan geri dönüş kaybı davranışı için deney sonuçları)

3.2. Short Circuit Case (Kısa Devre Durumu)

In this case, microstrip lines perpendicular to the direction of the vertical lines are placed, and the return loss behaviors are obtained depending on the various locations. The fault locations are changed by moving the horizontal tape to seven different locations (Fig. 10).

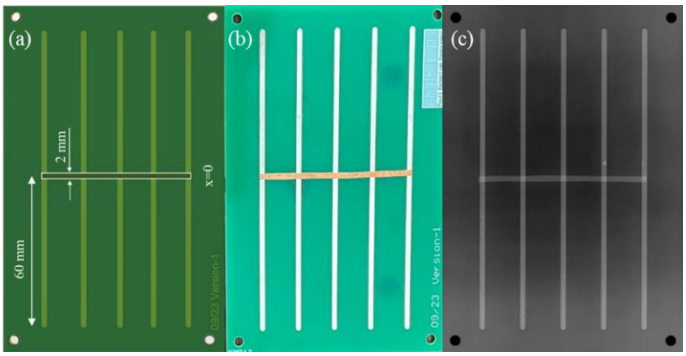

Figure 10. The design representation of the PCB (a), image of the PCB with short-circuit defect at x=0 (b), and X-ray image of the PCB with short-circuit defect at x=0 (c).

The results are given in the figure below (Fig. 11) and the magnitude and frequency values corresponding to the location of the faults are tabulated for comparison.

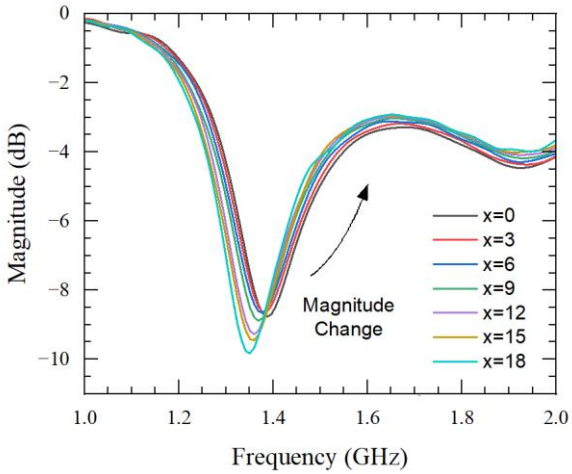

Figure 11. Simulation results for the Return Loss Behavior with respect to different locations of short circuits (Kısa devrelerin farklı konumlarına göre geri dönüş kaybı davranışı için simülasyon sonuçları)

As seen in the figure above, the location of the short circuit fault causes magnitude changes similar to the open circuit case. In addition, all short circuit cases are classified at a frequency range lower than open circuit results, which makes it possible to easily distinguish the fault type. Experimental measurement results obtained using the VNA are given in the following figure for all short circuit cases. As expected from the simulation, the magnitude values of the return loss data and the resonance frequency change depending on the fault location.

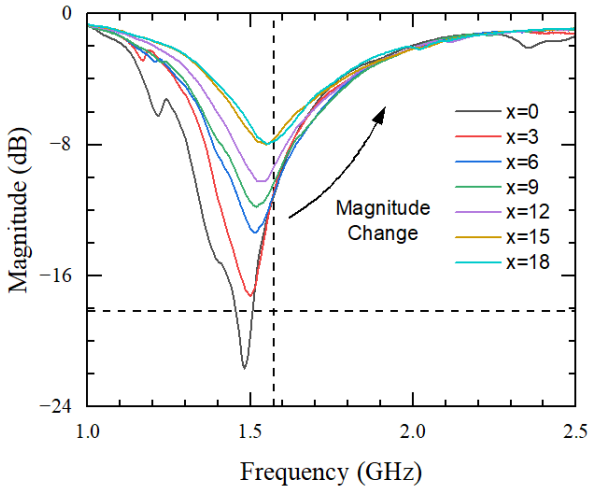

Figure 12. Experiment results for the Return Loss Behavior due to different locations of open circuits (Açık devrelerin farklı konumlarından kaynaklanan geri dönüş kaybı davranışı için deney sonuçları)

Experimental measurement results obtained using the VNA are given in the figure above for all short circuit cases (Fig. 12). As observed in the simulation, the magnitude values of the return loss data and the resonance frequency change depending on the fault location in the experimental study. It can be seen that the resonance frequency varies between 1.4 – 1.5 GHz band for short circuit case, while these values are between 1.5 – 2.0 GHz band for the open circuit case. For both cases, the bands to be used for the sensing operating are sufficient enough to have high accuracy in the measurements compared to the studies in the related literature. Studies focusing on the non-destructive testing of PCB faults are generally based on image/video processing techniques using several methods, such as YOLO. On the other hand, the proposed design only requires a network analyzer and a testing cable rather than having a complex testing structure. The accuracy of the tests performed in a study using image processing is around 75-80 % for open and short circuit cases [12]. However, such detection can be made using the proposed design with almost 1mm sensitivity with distinct separation and detection of PCB faults using a non-expensive antenna structure.

4. CONCLUSIONS

In conclusion, the designed structure is evaluated both theoretically and experimentally for various defect scenarios, and results are validated in terms of the working mechanism of the proposed design within 1.5 - 2.0 GHz frequency window. The designed metamaterial based circular patch antenna can be used successfully to determine not only the fault type (open, short circuit in our case) but also the location of the fault within mm-range on the PCB board. Depending on the fault location, the resonance frequency as well as the return loss magnitude (S11-dB) variation from -40dB to -16 dB around 1.5 GHz can be used for the sensing operation on PCB faults. The structure is designed so that it can be optimized easily to any other frequencies for PCBs with different wiring types and sizes. Even though only open and short circuit faults are investigated in this study, other common types of faults seen on PCBs can also be studied using the same structure in future studies. This proposed approach offers a non-destructive, rapid, and accurate all-signal-processing-based measurement method compared to the state-of-the-art solutions. A follow-up work shall include other aforementioned defect types with controllable factors such as size, location, and quantity. Also, future studies ought to include the other common PCB defect types (e.g., soldering

defects, missing holes) etc.) as well as combining two individual defects to assess the capability of the presented technique. As a result, the developed design can be used for quality control of PCB production plants along with other related industries to detect defect types and locations.

REFERENCES (KAYNAKLAR)

1. W. Jillek, W. Yung, Embedded components in printed circuit boards: a processing technology review. International Journal of Advanced Manufacturing Technologies, 25: 350–360, 2005.
2. A.C. Marques, J.-M. Cabrera, C.F. Malfatti, Printed circuit boards: A review on the perspective of sustainability, Journal of Environmental Management, 131: 298-306, 2013.
3. K.P. Anoop, N.S. Sarath, V.V. Sasi Kumar, A review of PCB defect detection using image processing, International Journal of Engineering and Innovative Technology 4(11): 188-192, 2015.
4. H. Rau, C-H. Wu, Automatic optical inspection for detecting defects on printed circuit board inner layers, The International Journal of Advanced Manufacturing Technology, 25: 940-946, 2005.
5. W. Dai, A. Mujeeb, M. Erdt, A. Sourin, Soldering defect detection in automatic optical inspection, Advanced Engineering Informatics, 43: 101004, 2020.
6. N. Asadizanjani, S. Shahbazmohamadi, M. Tehranipoor, D. Forte, Non-destructive pcb reverse engineering using x-ray micro computed tomography, International Symposium for Testing and Failure Analysis (ISTFA), 1-5 November 2015, Oregon, USA.
7. Y. Zhou, M. Yuan, J. Zhang, G. Ding, S. Qin. Review of vision-based defect detection research and its perspectives for printed circuit board, Journal of Manufacturing Systems, 70: 557-578, 2023.
8. G. Mahalingam, K. M. Gay, K. Ricanek. Pcb-metal: A pcb image dataset for advanced computer vision machine learning component analysis, 16th International Conference on Machine Vision Applications (MVA), 27-31 May 2019, Tokyo, Japan.
9. J. Schmitt, J. Bönig, T. Borggräfe, G. Beitinger, J. Deuse. Predictive model-based quality inspection using machine learning and edge cloud computing, Advanced Engineering Informatics, 45: 101101, 2020.
10. C.A. Balanis, Antenna theory analysis and design, 3rd Ed., John Wiley & Sons, New Jersey, 2005.
11. V.G. Veselago, The electrodynamics of substances with simultaneously negative values of ε and μ, Soviet Physics Uspekhi, 10, 509-514, 1968.
12. V. Kaya, İ. Akgül, Detection of defects in printed circuit boards with machine learning and deep learning algorithms, European Journal of Science and Technology, 41: 183-186, 2022.